

AD-A063 307

ENVIRONMENTAL RESEARCH INST OF MICHIGAN ANN ARBOR
REMOTE SENSING INVESTIGATION FOR BEACH RECONNAISSANCE. BEACH SA--ETC(U)
AUG 78 C F DAVIS, R A SHUCHMAN, G SUITS N00014-74-C-0273
ERIM-108900-12-F NL

UNCLASSIFIED

1 OF 1
AD
A063307



END
DATE
FILMED
3--79
DDC

108900-12-F

LEVEL II

12

Final Report

BASIC REMOTE SENSING INVESTIGATION FOR BEACH RECONNAISSANCE

Beach Sand Environment Task

C.F. DAVIS, R.A. SHUCHMAN, G.H. SUITS

AUGUST 1978

AD A063307

DDC FILE COPY

DDC
RECEIVED
JAN 17 1979
C

This document has been approved
for public release and sale; its
distribution is unlimited.

Geography Branch
Office of Naval Research
Arlington, VA 22217
Contract No. N0014-74-C-0273
Technical Monitor: Mr. Hans Dolezalek

ENVIRONMENTAL
RESEARCH INSTITUTE OF MICHIGAN
FORMERLY WILLOW RUN LABORATORIES, THE UNIVERSITY OF MICHIGAN
BOX 8618 • ANN ARBOR • MICHIGAN 48107

79 01 16 019

10 Carl F./Davis, Robert A./Shuchman
Gwynn/Suits

9 Final rept.
1 Jan 74-28 Feb 78

TECHNICAL REPORT STANDARD TITLE PAGE

1. Report No. 103900-12-F	2. Government Accession No.	3. Recipient's Catalog No.	
4. Title and Subtitle Final Report, Remote Sensing Investigation for Beach Reconnaissance, Beach Sand Environment Task	5. Report Date August 1978		6. Performing Organization Code
7. Author(s) C. Davis, R. Shuchman, G. Suits	8. Performing Organization Report No. 14 ERIM-108900-12-F		9. Work Unit No.
9. Performing Organization Name and Address Environmental Research Institute of Michigan Post Office Box 1618 Ann Arbor, Michigan 48107	11. Contract or Grant No. 15 N00014-74-C-0273		10. Type of Report and Period Covered Final 1-1-74 to 2-28-78
12. Sponsoring Agency Name and Address Geography Branch Office of Naval Research Arlington, Virginia 22217	14. Sponsoring Agency Code		
15. Supplementary Notes The technical monitor for this contract was Mr. Hans Dolezalek			
16. Abstract A review of the Beach Sand Environment task to date is given together with a description of a new sand reflectance model, AQUASAND. The AQUASAND model is a modification of the Suits radiative transfer canopy directional reflectance model. The model is used to generate artificial sand reflectance spectra whose parameters are user controlled. The spectra are subsequently used to develop an algorithm to predict mineralogy, moisture, and grain size of sands from input reflectance spectra. The problem of correct model input related to iron-staining of sand grains is addressed and solved. Using the proper iron-staining input the model is verified on 7 diverse beach types with varying moisture contents. The preliminary development and evaluation of a mineralogy, moisture and grain size algorithm is reported. A multistage regression framework appears to be the most productive type of algorithm.			
17. Key Words Beach Reconnaissance Remote Sensing Beach Sand Modeling Multispectral Scanner		18. Distribution Statement Distribution of this document is unlimited.	
19. Security Classif. (of this report) UNCLASSIFIED	20. Security Classif. (of this page) UNCLASSIFIED	21. No. of Pages 39 text + 5 prelim.	22. Price

407 903

39 01 16 018

gwr



PREFACE

The work described in this report was conducted by the Infrared and Optics Division of the Environmental Research Institute of Michigan (ERIM). The work was supported by the Office of Naval Research Geography Branch under Contract No. N00014-74-C-0273. The technical monitor was Mr. Hans Dolezalek.

Mr. Fred Thomson was principal investigator for the overall ONR contract, while Mr. Robert A. Shuchman acted as task leader for the Beach Environment study; the subject of this report. Mr. Carl F. Davis carried out the computer processing and analysis, while Dr. Gwynn Suits provided modeling expertise.

ACCESSION for

Whole Section

Half Section

UNIT

NO

BY

DATE

A

TABLE OF CONTENTS

	Page
1.0 BACKGROUND AND SUMMARY	1
2.0 TECHNICAL DISCUSSION	5
2.1 MODEL VERIFICATION	5
2.2 ALGORITHM DEVELOPMENT	12
3.0 CONCLUSIONS AND RECOMMENDATIONS	20
APPENDIX A. AQUASAND: A BEACH REFLECTANCE MODEL AND VALIDATION TEST	21
A1.0 INTRODUCTION	23
A2.0 MODELING	23
A2.1 REFLECTANCE MODELING CONCEPTS	24
A2.2 OPTICAL PROPERTIES OF SAND COMPONENTS	25
A2.3 MODEL DESCRIPTION	26
A3.0 RESULTS	29
A4.0 SUMMARY	29
APPENDIX B. SIMULATION OF MOISTURE VARIATION IN THE AQUASAND MODEL	36
REFERENCES	39

LIST OF TABLES

	Page
1. BEACH SAND CONSTITUENTS	8
2. SPECTRAL BANDS USED IN ALGORITHM DEVELOPMENT	13
3. GRAIN SIZE AND MOISTURE CONTENT OF AQUASAND GENERATED SANDS	15
A.1. BEACH SAND CONSTITUENTS	31

LIST OF FIGURES

<u>FIGURE</u>	<u>TITLE</u>	<u>PAGE</u>
1	Comparison of model generated and spectrally measured reflectances for seven common beach types	9
2	Two dimensional separation of moisture and grain size for a single mineralogy	16
3	Flow diagram for mineralogical, moisture, and grain size prediction algorithm	19
A1	Cross section of sand layers	31
A2	Diagram of model flow	32
A3	Plot of the absorption and scattering for carbonate in the .4 to 2.4 μm region	33
A4	Comparison of model generated and spectrally measured reflectances for seven common beach types	34
A5	Two dimensional separation of moisture and grain size for a single mineralogy	35

BACKGROUND AND SUMMARY

A program in coastal dynamics has been developed under the guidance of the Department of the Navy, Office of Naval Research. Working for this program are numerous researchers who are attempting to model coastal processes based on field collected data. It is the purpose of the Beach Environment Task to determine which beach features are of interest to the researchers active in the coastal dynamic program of the ONR and to determine if these features can be detected by an airborne remote sensing system.

The ability to remotely estimate composition of surface terrestrial materials has been demonstrated by many workers, and these results may have direct transfer value to beaches, where the composition is similar to that studied by geologists. The most prominent reports in this area have been by Vincent [1,2], Vincent and Thomson [3], and Vincent, Thomson, Watson [4]. These authors have explained the physical and optical properties of various rock and soils types as well as demonstrated the capabilities of a thermal infrared scanner in accurately classifying silica-containing soil and rock outcroppings and areas with surface iron stain. Discrimination is generally based on either atomic or ionic absorption in the shorter wavelengths (0.35 to 2.5 μm) and by lattice absorption at longer wavelengths (8-14 μm reststrahlen bands in silicate and carbonate minerals). These effect the spectral reflectance or emittance of materials.

Reststrahlen spectral emissivity variations with surface moisture have been studied by R.D. Watson [5]. He determined that as the thickness of water increased from 0 to 30 μm on a polished quartz slab, emittance increased at the principal quartz reststrahlen wavelengths of 8.5, 9.0, and 12.5 μm . This may be an important way to detect sample moisture content, and the effect will almost certainly influence compositional maps made of wet areas using the techniques reported by Vincent.^[1,2]

Another qualitative observation is that the size of silicate mineral grains affects the reststrahlen emissivity features. Hovis and Callahan [6] have demonstrated qualitatively that when the grain size of a sample is reduced from a solid sample to particles with diameters of 1-2 mm, 0.105-0.250 mm, and less than 0.038 mm, the measured reflectance progressively increases. Hunt and Vincent [7,8] have attempted to explain this phenomena in terms of a specular surface reflectance component (R_s) and a reflectance component which is due to radiation that has been transmitted through part or parts of the sample before re-emerging (R_v). The total sample reflectance is the sum of R_s and R_v . Further, the ratio R_s/R_v depends on grain size. Because R_s and R_v depend differently on the absorption coefficient, a . Thus, the reflectance or emittance of the sample will depend on grain size.

Because of the promising research described above ERIM began, in 1974, to relate grain size, degree of sorting, composition, and water content of beach sands to the spectral properties in the visible, reflective infrared, and thermal infrared regions. The objective was to find quantitative relationships between the spectral reflectances of beaches and their physical properties. During the first two years of the program, 50 beach sand samples from a variety of environments were collected. These samples were analyzed in terms of mineralogy, grain size, degree of sorting and degree of iron staining. In addition the spectral reflectance of each was determined in the 0.35 to 2.5 μm range using the Cary 14 spectrophotometer. A number of different moisture contents were used to simulate different regions in the land/water interface. Thermal infrared measurements were made in the 8-14 μm band on some of the sand types, however, further analysis was restricted to visible and near IR wavelength because of moisture attenuation in this region.

Several regression equations were developed at the end of the second year in an effort to predict grain size and moisture from spectral

data. Among them, a two channel moisture algorithm was developed which resulted in a coefficient of variation, $R^2 = 0.79$ and a standard error of 4.5%. Another moisture algorithm that used five spectral channel ratios was capable of predicting moisture content with a standard error of 4.0% and a R^2 of 0.86. Relative to grain size, one algorithm using 10 ratios was found capable of predicting the Wentworth grade scale of beach sands with an R^2 of 0.83. Although the results appear very good, the physical reasoning for the spectral channel selection and success of these algorithms was felt to be somewhat in doubt. In addition the large number of factors in the regression coupled with the relatively small data set reduced the significance of the results. These equations did, however, show the feasibility of developing an algorithm which could successfully predict moisture and grain size from spectral data.

In order to better control the variable parameters of beach sands and to more economically create the necessary data sets, work began in the third year on an adaptation of the Suits radiative transfer vegetative canopy model to the beach sand situation. The initial model, SANDREF, was verified by the end of the third year on two dry sands; a carbonate type and a pure quartz type. In the process of developing this unique modeling approach, the scattering coefficient (s), forward scattering (FS), and absorption coefficient (a) of sixteen common beach forming minerals were derived. This was the first time such a measurement had been achieved for these minerals. In order to develop these parameters three thin sections of each mineral of interest had to be cut. Each section had to be slightly thinner than the one before it. Using the reflectance and transmittance of each of the three thin sections, an iterative curve fitting procedure was used to develop the a , FS, and s parameters. These parameters were then used to predict the reflectance and transmittance of a given mineral at any desired thickness. The reflectances and transmittances were then entered into the SANDREF model.

After SANDREF was proven to work, it was modified to utilize moisture input to simulate the spectra of sand which contains water. The new program, called AQUASANDREF, included a moisture algorithm. The two modeling programs were then combined at the beginning of the fourth year into a single all-purpose program called AQUASAND. This composite program can theoretically handle any beach sand situation. It should be stated that the AQUASAND model is not designed to predict sand parameters from reflectance spectra but rather to generate spectra from known parameters. These spectra, in conjunction with measured spectra may be used to generate a predictive algorithm.

Specifically, the following accomplishments were made in year four:

- (1) A new method of modeling the iron-stain frequently found as a coating on sand grains, was developed.
- (2) The two models, AQUASANDREF and SANDREF, were combined and shortened into a much more efficient form (AQUASAND) for beach sand modeling. This version will handle modeling for both wet and dry sands.
- (3) A total of 7 diverse beach types were modeled successfully using separate mineralogical and moisture input to the new AQUASAND model.
- (4) Development of an algorithm to predict mineralogy, moisture, and grain size was begun using modeled data obtained from AQUASAND.

TECHNICAL DISCUSSION

As mentioned previously the modeling concept utilized in the third year of the ONR effort was verified on two beaches with relatively simple mineralogy and moisture content. This year, the dry model, SANDREF, was modified to utilize moisture input to simulated sand spectra which contained water. This new program called AQUASANDREF, was then combined with SANDREF into a single all-purpose program called AQUASAND.

AQUASAND was tested this year on a greater range of complex beach types - those that contain a greater variety of minerals in addition to varying moisture contents. Given in appendix A of this report is a copy of a paper entitled "AQUASAND: A Beach Reflectance Model and Validation Tests." This paper [9] presented at the Fifth Canadian Symposium on Remote Sensing of the Environment, summarizes fourth-year ONR results. A complete description of the AQUASAND model is given in this paper and, thus, will not be repeated in this section. The paper does not discuss the moisture algorithm developed for use in AQUASAND, however, a description of this algorithm is given in appendix B of this report.

2.1 MODEL VERIFICATION

One parameter that has a great effect on the reflectance of some beach sands is iron staining. In general, iron staining tends to reduce the overall reflectance of a sand. In addition, iron staining exerts a strong influence on the shape of the sand reflectance curve due to its absorption characteristics [10]. This absorption depends, to a great degree, on the oxidation state and hydration state of the iron. Unlike the other minerals we used, an iron stain cannot be modeled as being granular since, in nature, it appears as a coating on other mineral grains. Therefore, it was necessary for us to try other methods of expressing the stain so as to provide correct input to the model.

Our first approach was to artificially coat a glass surface with an iron stain and subsequently measure the reflectance and transmittance of this plate. The glass plates used were determined to be optically clear in the wavelength range of interest (0.35-2.5 μm) and as such they resembled quartz with an iron coating. This iron stain proved to be insufficient since the proper coating thickness, hydration state, and oxidation state of the iron could not be controlled accurately. The reflectance and transmittance spectrum obtained from the iron stained plates differed substantially from each other and, unfortunately, none seemed to correctly model the iron reflectance found in sand.

Because of this negative result another approach was taken. The reflectance of an iron stained quartz sand, BA1, [11] was measured on a Beckman DK-2A spectrophotometer. The Beckman, like the Cary 14 spectrophotometer is an instrument which is capable of continuously scanning reflectances or transmittances in the 0.30 to 3.0 μm range. It differs from the Cary 14 in that it has only an analog chart recorder rather than a digital recording capability. It has been found in the past that the Beckman is more accurate for determining hemispherical transmittance measurements due to the detector locations within the integrating sphere. Also, when digital recording is not essential the Beckman is usually employed because of its relative ease of operation as compared to the Cary 14. Following the initial measurement, the sand was bleached with nitric acid for three days to remove any iron stain from the grains. Prior to any measurements all the carbonate was removed from the sand manually since the nitric acid would have dissolved this together with any iron stain. (Removal of carbonate between the iron-stained and the non-iron-stained spectral measurements would, of course, have altered the reflectance spectrum independent of the iron.) After bleaching, the reflectance of the sand was remeasured. Any difference between the first and second measurement was assumed to be absorption (α) due to iron staining. The shape of the iron stain transmittance (τ) curve was expected to be:

$$\tau_{\text{Fe(shape)}} \approx 1 - \alpha_{\text{Fe(shape)}}$$

since the reflectance from the iron itself was assumed insignificant. This means that the color due to iron staining is related to light which is transmitted through the stain from below, not light which is reflected directly from the iron surface.

To verify this reasoning, a number of sand grains were masked into a black background so that only light which passed through the iron stained quartz was transmitted. The transmittance was then measured on the Beckman DK-2A spectrophotometer. As expected, the transmittance curve compared favorably to the reflectance spectrum described above supporting the contention that iron stain reflectance is negligible.

Since quartz has essentially no spectral shape, the transmittance spectrum we obtained was assumed to be due entirely to iron stain except for an 8% drop due to surface reflection in quartz. These transmittance values were then normalized such that 92% transmittance equaled an iron transmittance of 1 and 0% transmittance equaled an iron transmittance of 0. We were then able to multiply this "iron staining fraction" to any mineral we chose to simulate an iron stain on that mineral.

In order to fully verify the model, and the new iron input, seven beaches were chosen of differing mineralogies, grain sizes, and moisture contents. The spectra for these beaches were, in all but one case, among the 50 samples measured in the first and second year of the ONR effort. As such a full description of the sands is given in report no. 108900-3-T. The composition of the seven beaches selected for model verification along with their mineralogical and physical input parameters used in AQUASAND are given in Table 1. Figure 1 shows the AQUASAND generated reflectance curves (in the 0.4-2.5 μm region of the spectrum) for the respective beaches. Superimposed on each of the curves is the actual spectrum of the beach as measured using ERIM's Cary 14 spectrophotometer.

The first beach modeled was a carbonate type (see Figure 1). This sand is somewhat different from other beaches in that the individual grains tend not to be spherical in shape but rather appear as oblong plates. This is related to their origin as extoskeletal fragments derived from

TABLE 1
BEACH SAND CONSTITUENTS

<u>SAND</u>	<u>MEAN GRAIN SAND</u>
1. Carbonate	1 mm
99% Carbonate	
1% Organics	
2. AD2	.38
98% Quartz	
2% Feldspar	
3. BA1	.40
98% Quartz	
2% Feldspar	
4. EA2	.28
90% Quartz	
6% Feldspar	
2% Kaolinite	
2% Opaques	
5. D-Dune HI	.19
95% Quartz	
5% Feldspar	
6. MX2	.22
98% Quartz	
2% Carbonate	
7. HA1	.32
55% Quartz	
28% Feldspar	
4% Kaolinite	
13% Opaques	

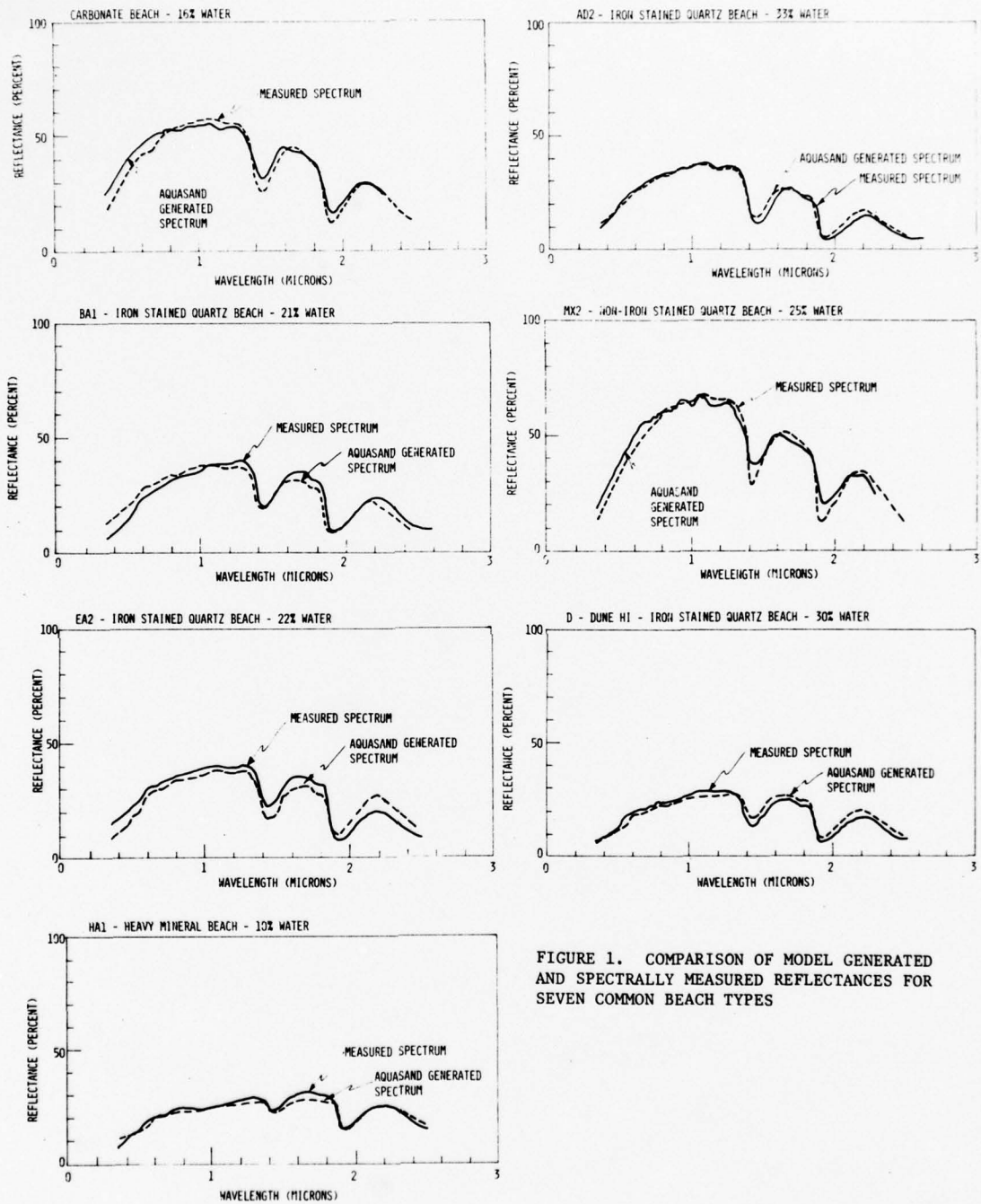


FIGURE 1. COMPARISON OF MODEL GENERATED AND SPECTRALLY MEASURED REFLECTANCES FOR SEVEN COMMON BEACH TYPES

marine organisms. The horizontal component for this beach was much greater than the vertical component due to the grain shape. In this context the horizontal component refers to that portion of the sand grain surface which is parallel to the beach surface while the vertical component is the corresponding portion which is orthogonal to the beach surface. (For a complete discussion of the AQUASAND model see appendix A.) Because of the nonspherical nature of carbonate grains they were entered into the model as being plates which were 1 mm in length and width and 0.25 mm in depth. Using this grain size input coupled with 16% water the modeled spectrum closely resembled the actual measured spectrum.

Representing the iron-stained Atlantic beaches, AD2 was chosen as the model test. This beach is reasonably well sorted and moderately iron stained. It provided the first test for the new iron stain input. Input to the model included 50% clear quartz, 30% polyquartz (representing frosted quartz), 5% carbonate and 15% iron-stained quartz. The minerals were inputted as spherical grains; 0.38 mm in diameter. This input together with a water content of 25% produced an excellent fit to the actual measured spectrum.

The Delaware Bay beach (BA1) is an alluvial sand of continental origin. In general the mean grain size is larger for this type of sand than its marine counterpart (A beaches). It is a moderately iron stained sand and has virtually no carbonate, unlike the A beaches. Based on measured data, input to the model included 55% clear quartz, 30% polyquartz, 9% iron-stained quartz, 5% opaques and 1% orthoclase feldspar. A grain size of 0.40 mm was entered for all minerals in addition to a moisture content of 21%. The model fits the actual measured spectrum quite well, however, there is roughly a 5% difference in reflectance in the region between 0.35 and 0.7 μm .

MX2 represents a non iron-stained quartz beach such as that found on the Gulf of Mexico coast. It exhibits high reflectance even with a high moisture content. The sand is extremely well sorted, and has very spherical grains. It is virtually pure quartz except for a small amount of organism related carbonate and dark opaque organic matter. The model input included 97% polyquartz, 2% carbonate and 1% opaques at a grain size of 0.22 μm . Water input to MX2 was 25% and the resulting fit was very good. There are some spectral features between 0.8 and 1.2 μm which the

model failed to represent, however, they seemed to be an artifact of this beach only and were not consistently represented in the other Mexico beaches.

The EA2 and D-dune beaches were both continental beaches collected on the shore of Lake Michigan. The primary differences between the two were a greater amount of opaque rock fragments and substantially more iron staining in the D-dune beach. Also the D-dune beach was modeled with a moisture content of 30% while the EA2 beach had 22%. As with the other beaches these moistures corresponded to the previously measured values obtained in the first two years of the ONR program. These differences yield a depressed reflectance spectrum for the D-dune beach relative to the EA2 beach and the model successfully showed this. The D-dune beach was modeled using 70% clear quartz, 20% iron stained quartz, 5% carbonate, and 5% opaques at a grain size of 0.17 mm. The EA2 beach had 60% clear quartz, 20% iron stained quartz, 3% opaques, 7% polyquartz and 10% orthoclase at a grain size of .28, as input. The model results are good for both beaches particularly related to the sudden drop in reflectance around 0.6 μ m. This appears to be related to iron stain and is characteristic of the Michigan beaches within our data set.

HA1 was chosen as an example of a heavy mineral beach (particle density >2.65). "Heavy mineral" is a loose definition we have affixed to any beach which shows a strongly depressed reflectance spectrum, particularly in the visible region. These beaches usually exhibit the property of having higher reflectance in 1.2-1.8 μ m region than in the visible (except for the water bands). In the case of HA1 the depressed reflectance spectrum seems to be related to a high percentage of opaque rock fragments in the beach (12.3%). These rock fragments were inputted to the model as opaque grains regardless of their mineralogy since their low reflectance functionally suppresses any spectral characteristics.

The input to the model included 50% clear quartz, 33% iron stained quartz, 10% ilmenite, and 70% orthoclase at a grain size of 0.32 for HA1. The spectral fit is very good except for a miscalculation of spectral shape in the 0.35 to 0.55 μ m region.

Notice that the mineralogical input to the model does not, in all cases, correspond exactly to the measured mineralogical percentages in the sand. This is probably due to many uncontrollable factors including random preference of one mineral over another during the reflectance measurements and subtle tendencies towards a grain size-mineralogy correlation in the samples. The important fact is that the model behaves correctly to changes in moisture and grain size once mineral inputs are determined.

In summary, the new iron-stain modeling concept allowed us to achieve good correlation between the actual measured reflectance spectra, and the model output for seven diverse beach sands. In addition the moisture input to the AQUASAND model is an excellent representation of the actual data in every case.

2.2 ALGORITHM DEVELOPMENT

With the model fully verified, work began on the development of a prediction algorithm for beach parameters. The initial plan called for using simulated multispectral scanner bands in some n dimensional system to create a classification structure for the three major parameters - mineralogy, moisture content, and grain size. It was determined that preliminary analysis should be accomplished in two dimensions to facilitate a simpler interpretation of the results. In addition, a single mineralogy, that of an AD2 beach, was used with the intention of separating mineralogy prior to moisture and grain size. Both single bands and ratioed bands were considered. Computer programs were developed which maximized the area separation of the data points in this two dimensional system since the number of potential two way combinations was too large to handle manually.

Fifteen potential channels were investigated (Table 2). These channels were chosen as being representative of a general scanner system. The breaks in channel coverage near 1.4 and 1.9 μm , are of course, related to

TABLE 2
SPECTRA BANDS USED IN PRELIMINARY
ALGORITHM DEVELOPMENT

<u>Band Number</u>	<u>μm Range</u>
1	.4-.45
2	.45-.5
3	.5-.55
4	.55-.6
5	.6-.65
6	.65-.7
7	.7-.75
8	.75-.8
9	.8-.9
10	.9-1.0
11	1.0-1.1
12	1.1-1.2
13	1.2-1.35
14	1.55-1.8
15	2.1-2.3

atmospheric water absorption. With the advent of active laser systems, the bandwidth is potentially much finer than is indicated in Table 2, but for our preliminary purposes this band composition was deemed sufficient.

Using the AQUASAND model, 12 different beach sand spectra of identical mineralogy were derived using variable moisture and grain size input. The combinations are given in Table 3. These spectra were then condensed into the appropriate bands using linear averages. These bands were then scattered against each other. For the single band situation 105 potential unique combinations were investigated. Of these, band 1 (0.4-0.45 μm) against band 10 (0.9-1.0 μm) provided the maximum separation of moisture and grain size (Figure 2).

The ratio case was somewhat more complex. Using 15 bands there were 105 potential ratios and 7560 possible unique combinations of the ratios in the two dimensional system. Maximum separation of grain size and moisture achieved with the ratio of band 10 to band 14 (0.9-1.0 μm /1.55-1.8 μm) on one axis and band 1 to band 14 (0.4-0.45 μm /1.55-1.8 μm) on the other (Figure 2). The ratioed situation was considered more favorable since it would tend to reduce effects of noise within the system when applied to actual scanner data.

As can be seen in Figure 2, separation of moisture and grain size was unambiguous for both the single band and the ratio case. Both were within the theoretical sensitivity of the scanner system although separation using ratios appears the better of the two. The ratio of band 1 to band 14 appears to increase with increasing grain size. This is evidenced by an increase in reflectance in the 0.4-0.45 μm band as grain size increases. The 1.55-1.8 μm band remains more or less stable with grain size changes. As moisture increases the reflectance in the 1.55-1.8 μm band decreases and hence the ratio, band 10 to band 14 increases. For both moisture and grain size, band 10 (0.9-1.0 μm) can be considered a reference in the ratio which is relatively stable as the parameters of interest vary.

TABLE 3
GRAIN SIZE AND MOISTURE CONTENT OF
AQUASAND GENERATED SANDS USING AD2 MINERALOGY

<u>Sand Number</u>	<u>Grain Size</u>	<u>Moisture %</u>
1	.38	4
2	.38	12
3	.38	20
4	.38	28
5	.60	4
6	.60	12
7	.60	20
8	.60	28
9	.95	4
10	.95	12
11	.95	20
12	.95	28

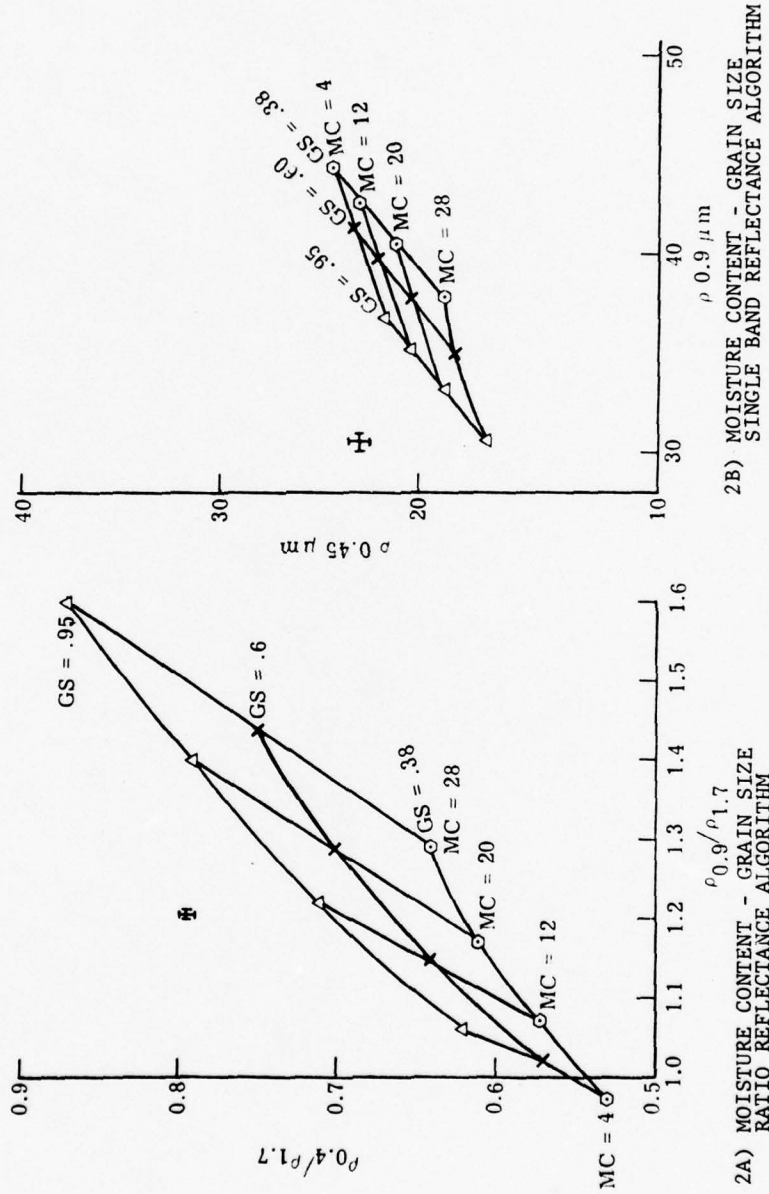


FIGURE 2. RATIO REFLECTANCE AND SINGLE BAND ALGORITHMS FOR SEPARATING MOISTURE AND GRAIN SIZE.

As a test of the robustness of this algorithm a Mexico beach mineralogy was generated using AQUASAND and the moisture and grain size were varied as before. The results showed the same relationship of changes, however, the absolute values of the ratios were substantially different; so different in fact that accurate prediction of moisture and grain size based on the AD2 algorithm would have been impossible. This outcome indicated that the mineralogical differences between Mexico Beach compositions and AD2 compositions would have had to have been broken down previously and two separate grain size moisture algorithms would be needed.

Assuming that Mexico Beach mineralogy was too unlike AD2 mineralogy to use in the AD2 algorithm it was decided that actual spectrally measured, A-beach data should be tested in the algorithm. As such the appropriate bands from the original ten A-beaches were tested using the AD2 algorithm. The results were not promising. Although the spectral response related to moisture was predictable, the spectral response due to grain size was not. The implication is that even subtle changes in mineralogy within the same geographic area are sufficient to overpower changes related to a moisture and grain size, particularly the latter.

A further difficulty with developing an algorithm along the lines described above is related to the definition of classification boundaries around the modeled points defined by moisture and grain size. Since the input is created by a model there is no inherent "noise" or variation such as that found in a natural system. As such, it is impossible to define an actual distribution of ratioed values related to a particular grain size moisture combination. One solution would be a nearest neighbor approach saying that an input point is classified as to moisture and grain size by the closest modeled point. This is probably insufficient since the relationships are non-linear. Another more suitable answer would be some kind of curvilinear interpolation between the modeled points, however, in any more than 2 or 3 dimensions this methodology would be

extremely difficult. In conclusion, the above procedure is not sufficient for our purposes.

Another approach to algorithm development would be the use of a stepwise procedure, and, at this time, such a route seems to be the most productive. The algorithm will consist of many equations proceeding from the most easily differentiable parameter, mineralogy, to the most difficult, grain size. The rationale is that by the time grain size must be determined, all other controllable parameters will be accounted for. The approach is shown visually in Figure 3.

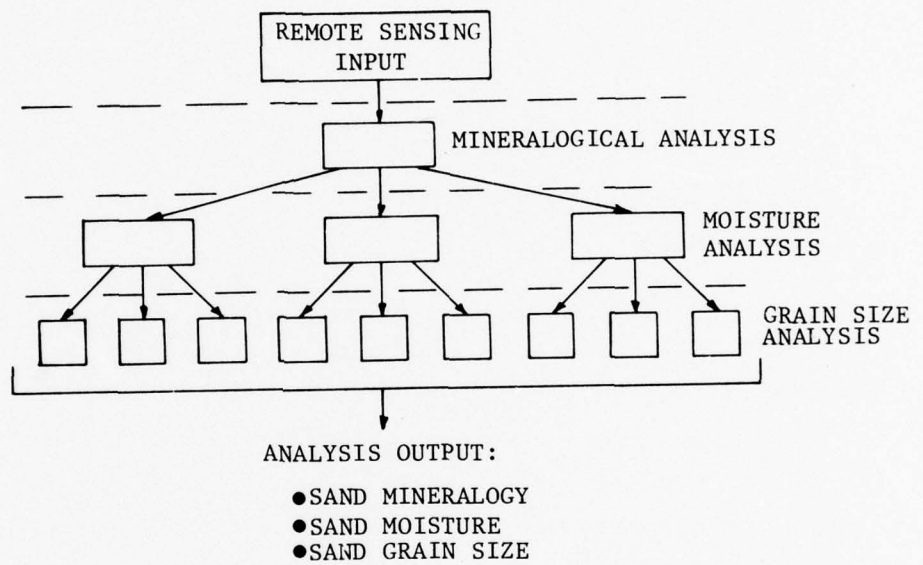


FIGURE 3. FLOW DIAGRAM FOR MINERALOGICAL, MOISTURE, AND GRAIN SIZE PREDICTION ALGORITHM

CONCLUSIONS AND RECOMMENDATIONS

At the present time the AQUASAND model appears to be functioning well. For seven diverse beach types the parameters and output seem to be an accurate representation of actual measured spectra. The concept of developing an algorithm to predict beach parameters from spectral data appears sound, however, grain size appears to be a very sensitive parameter which is easily overshadowed by extraneous variables. For a single mineralogy, however, separation of grain size and moisture was demonstrated using modeled data generated by AQUASAND.

The next logical move is to implement the composite algorithm approach described above. The first step in this computer algorithm will be a preliminary breakdown of the sand mineralogy into classes using a discriminant function of some type based on appropriate single bands or ratios. The second step will be a series of regression equations, one for each mineralogy to determine moisture content. The third and final analysis will be another series of regressions, one for each moisture, from which grain size will be determined. Obviously this could lead to a tremendous number of equations, however, several moisture contents may be able to use the same grain size regressions. Perhaps mathematical functions can be developed that describe the changes in the regression coefficients with moisture. If this is possible then simple modification of one regression equation for several moisture conditions is feasible.

In order to tie this algorithm development to the real world as much as possible, actual reflectance measurements made on the Cary 14 should be used to develop stage 1 and 2 of the algorithm. The data to develop the regressions related to grain size will have to come from the AQUASAND model.

APPENDIX A

AQUASAND: A BEACH REFLECTANCE MODEL AND VALIDATION TESTS

Paper presented at the Fifth Canadian Symposium on Remote Sensing of
the Environment, August 1978, Victoria, British Columbia, Canada

APPENDIX A

AQUASAND: A BEACH REFLECTANCE MODEL
AND VALIDATION TESTS*

R.A. Shuchman, G.H. Suits, C.F. Davis
Environmental Research Institute of Michigan
Ann Arbor, Michigan 48107

ABSTRACT

A new sand reflectance model called AQUASAND has recently been developed. This model, a modification of the Suits radiative transfer vegetation canopy directional reflectance model, accounts for the reflectance and transmittance of sand particulates in the .35 to 2.5 μm spectral range. The AQUASAND model also accounts for the influence of soil moisture within the sand. The model will ultimately determine the practical limits of remote sensing algorithms for determining physical and chemical properties of beaches.

The AQUASAND model uses, as inputs, the coefficients of absorption and scattering and the forward scattering fraction for each mineral comprising the beach sand (i.e., quartz, feldspar, kaolinite, etc.), the average number of grains (particles) per given volume from which average cross sections of each mineral type can be computed, void space, and the moisture depth profile of the beach to calculate the reflectance of the beach. ERIM, using its Cary 14 spectral reflectometer, measured the hemispherical transmittance and reflectance of sixteen common beach forming minerals at a number of prescribed thicknesses to obtain the needed coefficients and forward scattering fraction.

Additionally, ERIM used the same instrument to measure actual sand samples collected from fifty diverse beaches found on United States coastlines. These reflectance spectra were used to evaluate the AQUASAND model. The results are very encouraging showing good agreement between the actual beach spectra and the model results when the individual mineral components comprising the beach are correctly identified and inputted into the model.

The validated AQUASAND model (based on ten of the fifty actual beach samples) is currently being used to generate algorithms that

*This work is supported by the United States Office of Naval Research (ONR), Contract No. N0014-74-0273. Mr. Hans Dolezalek is the technical monitor.

predict grain size, moisture contents, and mineral composition using remotely sensed reflectance information in the .35 to 2.5 μm spectral range.

1.0 INTRODUCTION

This paper discusses a new radiative transfer model called AQUASAND. This model predicts the reflectance of beach sands in the .35-2.5 μm wavelength range of the electromagnetic spectrum. This newly developed sand reflectance model will ultimately determine the practical limits of remote sensing algorithms for determining physical and chemical properties of beaches.

The use of .35 to 2.5 μm radiation to determine physical and chemical properties of beaches is deemed feasible from the proven capability of mapping silicate minerals using reststrahlen techniques in the 8 to 14 μm spectral range, a procedure developed by Vincent and Thomson (1972) and earlier by Vincent and Hunt (1958). The .35 to 2.5 μm region of the spectrum is of interest for beach parameter sensing since water is relatively transparent in this region (unlike the 8 to 14 μm region) and beaches typically have high moisture contents.

2.0 MODELING

The capability of determining important physical properties of beach sands by remote sensing techniques depends upon the interaction of radiation with the constituent materials of the beach. Such interaction is certainly complex but, nevertheless, must follow the laws of nature. The purpose of making a mathematical reflectance model of this complex interaction is to achieve insight into the relationship between the remotely received signals and the physical properties of the beach sand that are of interest.

A mathematical model of a physical phenomenon is the result of incorporating the mathematical expressions of the laws of nature as they apply to a complex circumstance so that the conclusions drawn from the assembled expressions correspond to the physical results of an experiment under similar circumstances. Such a model requires experimental validation using a few but diverse circumstances in order to prove that the essence of the phenomenon is contained in the logic of the model. Once validation has been achieved, the model may be used as a readily available and inexpensive substitute for experiment under all circumstances within the scope of the circumstances of the validation experiments. In addition, the logical structure of the model provides the insight into the significant interaction processes so that more general conclusions may be drawn.

2.1 Reflectance Model Concepts

The most elementary model of sand reflectance is the simple plane mixtures model. The model employs the assumptions that all sand particles are opaque and are randomly mixed. The surface of the sand layer exposes sand particles in proportion to the product of their mean cross sectional area and the concentration of the particles in the sand mixture. Thus, the reflectance spectrum of the mixture is predicted to be the area weighted average of the reflectance spectra of the various minerals exposed at the sand surface. Multiple scattering between particles is assumed to be negligible and one surface particle is assumed not to obscure from view an adjacent surface particle.

This elementary model fails to achieve good accuracy because the transmittance of particles in a finely divided state may be quite large and multiple scattering of radiation between particles should be significant. In addition, the packing of grains in layers produces partial exposure at the surface so that line of sight to some particles will depend upon the direction of view. A more complex model is required to account for these effects.

The more complex model which is used in this work employs the identical concepts that are employed by the directional reflectance model for vegetative canopies (Suits, 1972). It may be hard to visualize off-hand that the interaction of radiation with a vegetative canopy is homomorphic with the interaction of radiation with sands because vegetation and sand hardly appear the same to the eye. Nevertheless, the essence of the reflection, transmission, and multiple scattering phenomena is the same concept for the optical parameters of the components that are involved as long as the wavelength is much smaller than the particles.

The first assumption of this model is that the scattering components are distributed more or less uniformly in horizontal layers where the mixture of component types may be different in the various layers. In a corn field, for example, the tassels always appear at the top, green healthy mature leaves appear in a middle layer and necrotic leaves appear usually near the soil. In sands, the action of wind and waves are likely to stratify mineral mixtures vertically and certainly moisture content varies with a vertical moisture profile. The division in layers is done in order to "quantize statistically what may otherwise be nearly a continuous distribution.

The second assumption is that the radiation field may be divided into two types of radiant flux -- specular and diffuse. The specular flux represents the radiation arriving from the source with rectilinear propagation and passes through the holes, cracks, and voids of the ensemble of randomly packed components without deviation.

The diffuse flux is derived from the specular flux and is that part of the specular flux which has been intercepted by a scattering component at least once and is scattered in both forward and backward directions. In a vegetative canopy, specular flux frequently reaches the soil level and appears as sun flecks on the soil. In a sand, specular flux diminishes exponentially to negligible proportions in only a few millimeters depth. Optically, the sand is infinitely deep. However, the diffuse flux is derived from the specular flux in the identical manner. The diffuse flux may penetrate much deeper into the sand than can specular flux.

The third model assumption is that the manner of scattering by mineral particulates can be adequately represented by replacing each mineral particulate with a set of equivalent Lambertian panels which have the same spectral transmittance and reflectance as does the component. This assumption defines a simplified scattering phase function which permits one to calculate ensemble reflectances in closed form. The form of the scattering phase function becomes significant when single scattering is the dominant phenomenon. Scattering by widely dispersed aerosols in the atmosphere (e.g., smoke and dust) exhibits detailed phase function effects. However, as the degree of multiple scattering increases, the detailed features of the scattering phase function are no longer significant. In both sands and vegetative canopies, multiple scattering effects dominate because of the high density of scattering components.

The fourth model assumption is that the diffuse flux moves generally vertically upward and downward with a Lambertian angular distribution as a first approximation. The reflectance of the ensemble is calculated using the method of self-consistent field with the specular and approximate diffuse flux as the illuminant of components. The ensemble reflectance is not necessarily Lambertian but is only approximately so. Both vegetation and sand meet this approximate criterion.

Because of the homomorphic relationship of radiative interactions with sand and vegetative canopies, the reflectance model previously developed for vegetation is applied to sand with the appropriate component properties for sand minerals substituted for vegetative canopies.

2.2 Optical Properties of Sand Components

The cross section view of a hypothetical sand layer containing two kinds of minerals is shown in Figure 1. The irregular shapes of the sand grains result in some more or less random, loose packing with many voids. These grains are to be replaced by a number of equivalent Lambertian panels which will intercept approximately the same amount of radiant flux as do the actual grains. The spectral reflectance and transmittance of the panels are to be the same as

the spectral reflectance and transmittance of the grains. Since these spectral properties may change with grain size or state of division, some means of calculating the appropriate spectral properties is required.

An auxiliary reflectance and transmittance model for mineral thin sections was developed in order to relate the inherent spectral properties which are characteristic of a mineral to the properties of that mineral in any state of division. Three characteristic bulk properties were taken to be sufficient for this purpose -- the spectral absorption coefficient, a , the forward scattering fraction, FS , and the scattering coefficient, s .

Radiation which penetrates a mineral may be absorbed and converted into heat energy depending upon the chemical composition of the mineral. A mineral which is internally homogeneous without inclusions and cracks will transmit radiation passing through it in accordance with the relation,

$$E(x) = E_0 e^{-ax}, \quad (1)$$

where $E(x)$ is the irradiance on a plane at depth x in the mineral,

E_0 is the irradiance on a plane inside the first surface,

a is the spectral absorption coefficient.

The spectral absorption coefficient will be a function of the wavelength of the penetrating radiation and will depend upon the chemical composition of the mineral. The spectral absorption coefficient is largely responsible for the spectral variations in mineral reflectance and transmittance.

The formation of minerals is a complex natural process so that minerals may not be optically homogeneous. Foreign materials are often formed in the interior of the mineral. Such features as fractures, gas bubbles, small crystals of associated minerals, and grain boundaries of anisotropic crystals create inhomogeneities within mineral bodies. These inhomogeneities reflect or scatter and deviate penetrating radiation from rectilinear propagation. A collimated beam of radiation which propagates rectilinearly through the body of a mineral will be diminished due to such scattering by the relation,

$$E(x) = E_0 e^{-sx}, \quad (2)$$

where $E(x)$ is the irradiance of rectilinear flux on a plane at depth x ,

E_0 is the irradiance of rectilinear flux at the first surface,

s is the scattering coefficient.

The radiation which is scattered will tend to propagate either deeper into the mineral -- forward scatter -- and contribute to transmittance or reverse direction and propagate back out of the mineral -- backscatter -- and contribute to reflectance of the mineral. The fraction of scattered radiation which continues deeper into the mineral is the forward scattering fraction, FS. The fraction of scattered radiation which reverses is then (1-FS). The scattering coefficient and the forward scattering fraction can be spectrally dependent but should not be the primary determinant of the spectral quality of a mineral.

These three optical properties of a mineral, a , s , and FS, are assumed to be independent of the thickness of the mineral. That is, the inhomogeneous structure and chemical composition of a mineral thin section is assumed to be evenly distributed so that a , s , and FS, are inherent properties characteristic of the kind of mineral and not the size of the mineral sample.

The auxiliary reflectance and transmittance model for mineral thin sections makes use of these three properties and the index of refraction of the mineral to yield the thin section transmittance and reflectance for any mineral thickness. The value of a , s , and FS, for each wavelength must be determined experimentally. However, these properties cannot be determined by direct experiment. Instead, a spectral reflectometer was used to measure the transmittance and reflectance of mineral thin sections having various thicknesses. Since a , s , and FS are presumably thickness invariant, the value of a , s , and FS may be determined by finding the value of a , s , and FS which, when used in calculating the transmittances and reflectances of thin sections having these various thicknesses, yield matching values for the reflectances and transmittances found experimentally. A computer iteration technique was used for this purpose.

Then spectral values of a , s , and FS for some of the common sand minerals have been tabulated. For certain opaque minerals, such as hematite and limonite, the values of a , s , and FS could not be determined. The transmittance and reflectance of these minerals are independent of grain thickness for all thicknesses that are likely to be found in sands. The reflectance and transmittance of pure, unstained clear quartz is due almost entirely to surface effects which are also independent of grain thickness.

The optical properties of sand components are determined and are introduced into the sand reflectance model. The spectral transmittance and reflectance of the equivalent Lambertian panels for each mineral are determined using the auxiliary reflectance and transmittance model for mineral thin sections where the thickness of thin section is the mean grain thickness for each mineral. The mean cross section of grains of each mineral type is multiplied by the corresponding number of such grains per unit volume for a given

beach sample and represents the scattering effect of the equivalent Lambertian panels.

2.3 Model Description

Figure 2 indicates the flow of information beginning with the raw experimental CARY transmittance (τ) and the reflectance (ρ) data and ending with the predicted reflectance spectrum for sand. As indicated previously, the needed input into the AQUASAND model are transmittance, τ , and reflectance, ρ , values for the individual minerals in a particular sand configuration. These τ and ρ values must be calculated for each particle size. Experimentally, τ and ρ spectra were determined for each mineral at given thicknesses. Some minerals which were opaque exhibited a negligible amount of transmittance. Iron stains were treated as separate minerals and experimental τ and ρ spectra were determined for them. These inputs are shown on Figure 2.

In order to predict τ and ρ 's for any particle size, properties independent of size can be determined. These properties previously discussed, are the forward scattering (FS), scattering coefficient (s) and the spectral absorption coefficient (a). The computer program calculates these coefficients for a given mineral using the experimental τ 's and ρ 's and the experimental thicknesses and the parameters of refraction (particle to air (RPA) and air to particle (RAP)).

These determinations of the fundamental a , FS, and S properties of sixteen common beach forming minerals in the $.35\text{-}2.5\ \mu\text{m}$ range are the first such measurements made to date. Figure 3 is a plot of a and S for a carbonate beach.

Once the absorption and scattering coefficients are determined, another computer program uses these coefficients coupled with the parameters RPA and RAP to predict τ 's and ρ 's for a given thickness. These predicted values are then used to model the sand.

The final program, AQUASAND, computes the reflectance of mixtures of minerals. The inputs to this program consist of the predicted τ 's and ρ 's for the minerals constituting the sand, the amount of iron stain, the depth of the sand, the reflectance of an infinite depth background underneath the sand, the particle cross sections and packing factors for the various minerals, the angle of illumination from a point source illuminator (or optional Lambertian source) and the angular position of the sensor and the percent moisture of the sand on a millimeter scale.

The output of AQUASAND is a predicted reflectance spectra of the sand for various configurations of illuminator position (θ) and sensor position (Φ, ψ). The AQUASAND program was derived from a program which predicted reflectances for a two layered vegetation canopy

with a background. Thus the sand can have two layers with different densities and grain sizes in each layer. A background material for the sand can also be specified. These properties of AQUASAND allow great flexibility for modeling various configurations such as thin sands, sand after a storm with a layer of organic matter or stones on top, etc.

3.0 RESULTS

Seven beaches of diverse mineralogy, moisture content, and grain size were selected for evaluation of the AQUASAND model. The beaches selected for model verification along with their mineralogical and physical parameters used as input into AQUASAND are given in Table 1. Figure 4 shows the seven AQUASAND generated reflectance curves (in the .4-2.5 μm region of the spectrum) for the respective beaches. Superimposed on each of the seven curves appears the actual spectrum of the beach as measured using the ERIM Cary 14 spectrophotometer.

These results are very encouraging, for although the absolute values of the curves differ, the overall shape and absorption bands seem to correspond remarkably well.

4.0 SUMMARY

The AQUASAND reflectance model has been satisfactorily evaluated. The model is currently being used to generate hypothetical sands, so that grain size and moisture prediction algorithms can be generated using remote sensed data.

A beach resembling the mineralogy of beach sample AD2 (see Table 1, and Figure 4) has been parametrically run with various moisture and grain sizes using AQUASAND. The generated spectral graphs similar to those shown in Figure 4 were then examined to determine optimum single or ratio spectral intervals to predict moisture and grain size.

A summary of that analysis is shown in Figure 5. The graph on the left of the figure shows ratio channels selected while the graphs on the right show single channels selected from AQUASAND parametrically varied results.

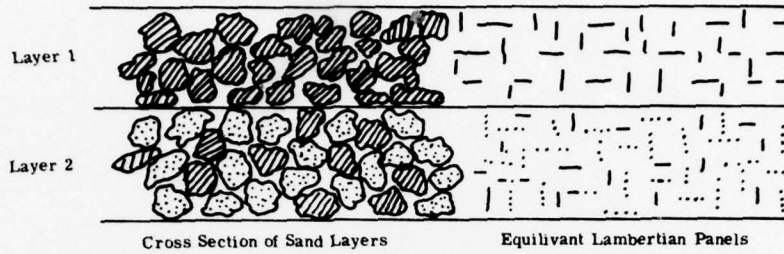
Currently AQUASAND is being used to generate beach sands where only one physical or chemical property is parametrically varied. Regression analysis is then applied to the AQUASAND results to obtain the finalized moisture and grain size prediction algorithms.

REFERENCES

G.H. Suits, The Calculation of the Directional Reflectance of a Vegetation Canopy, Remote Sensing of the Environment, Vol. 2, pp. 117-125, 1972.

Vincent, R.K. and G.R. Hunt, Infrared Reflectance from Material Surfaces, Applied Optics, Vol. 7, No. 1, 1958, pp. 53-59.

Vincent, R.K. and F.J. Thomson, Spectral Compositional Imaging of Silicate Rocks, J. Geophysical Res., 1972, pp. 2465-72.



Layer 1 is shown as consisting of grains of only one kind of mineral.
 Layer 2 is shown to consist of a mixture of two kinds of minerals.
 The equivalent Lambertian scattering panels are illustrated on the right.

FIGURE 1. CROSS SECTION OF SAND LAYERS

TABLE 1. BEACH SAND CONSTITUENTS

<u>Sand</u>	<u>Mean Grain Sand</u>
1. Carbonate 99% Carbonate 1% Organics	1 mm
2. D-Dune HI 95% Quartz 5% Feldspar	.19
3. MX2 98% Quartz 2% Carbonate	.22
4. BA1 98% Quartz 2% Feldspar	.40
5. EA2 90% Quartz 6% Feldspar 2% Kaolinite 2% Opaques	.28
6. AD2 98% Quartz 2% Feldspar	.38
7. HA1 55% Quartz 28% Feldspar 4% Kaolinite 13% Opaques	.32

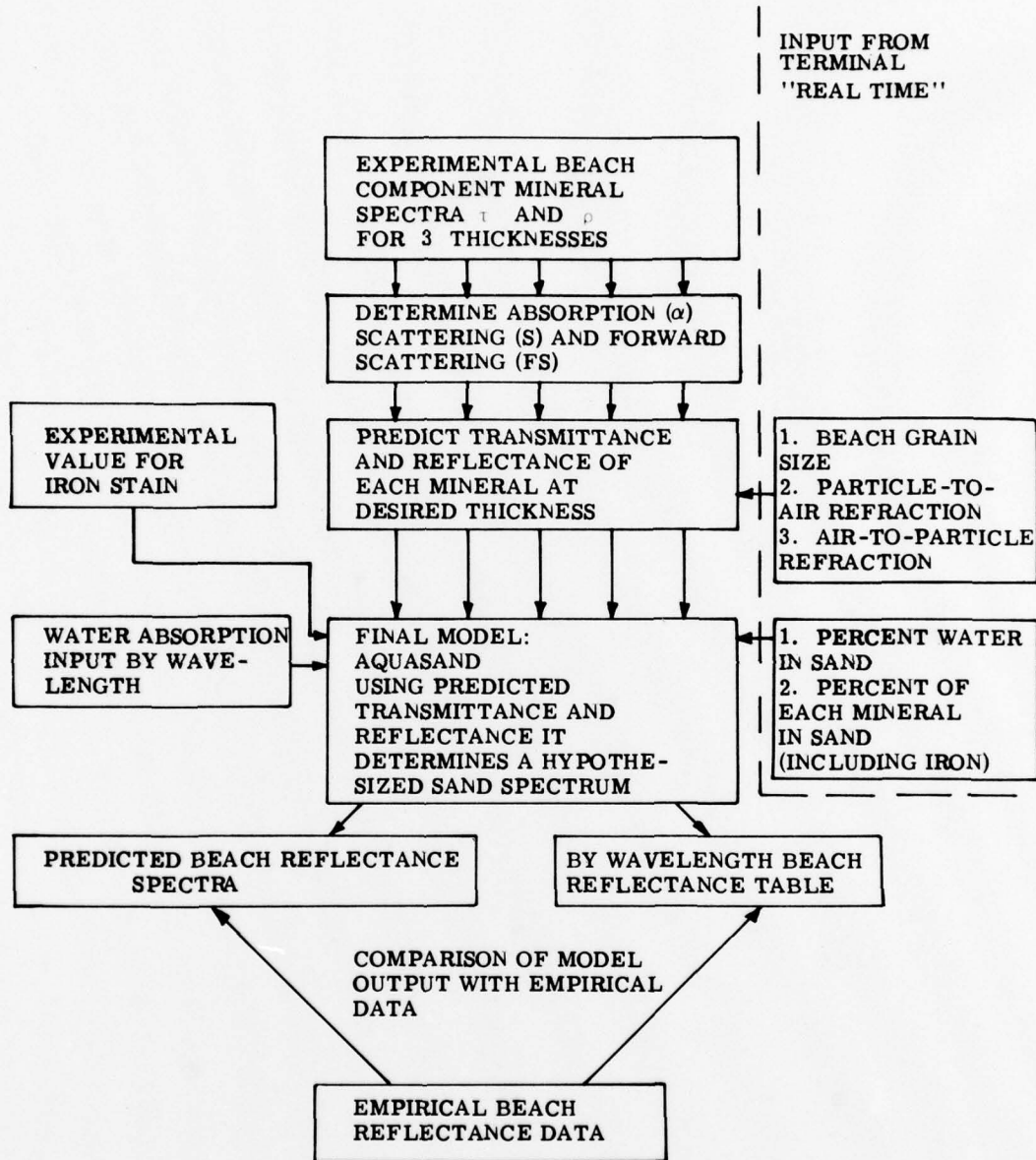


FIGURE 2. DIAGRAM OF MODEL FLOW

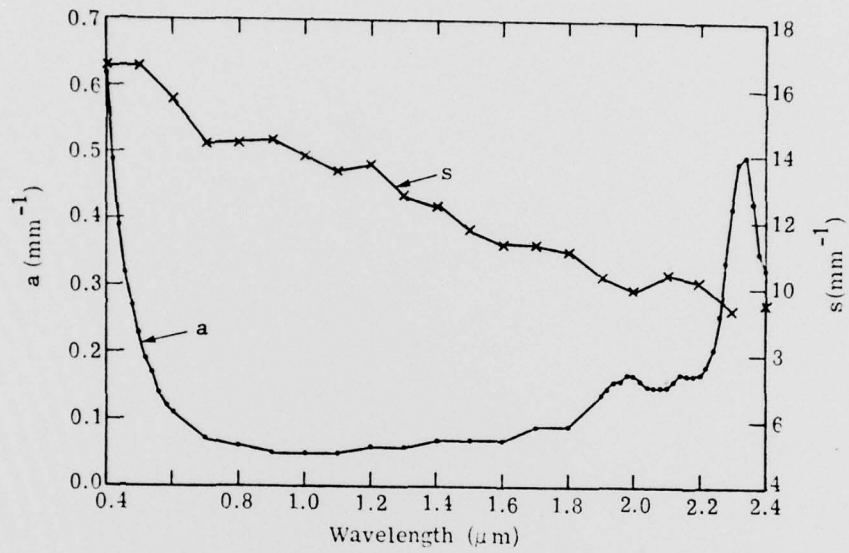


FIGURE 3. PLOT OF THE ABSORPTION COEFFICIENT (a) AND SCATTERING COEFFICIENT (s) FOR CARBONATE IN THE .4 TO 2.4 μm REGION

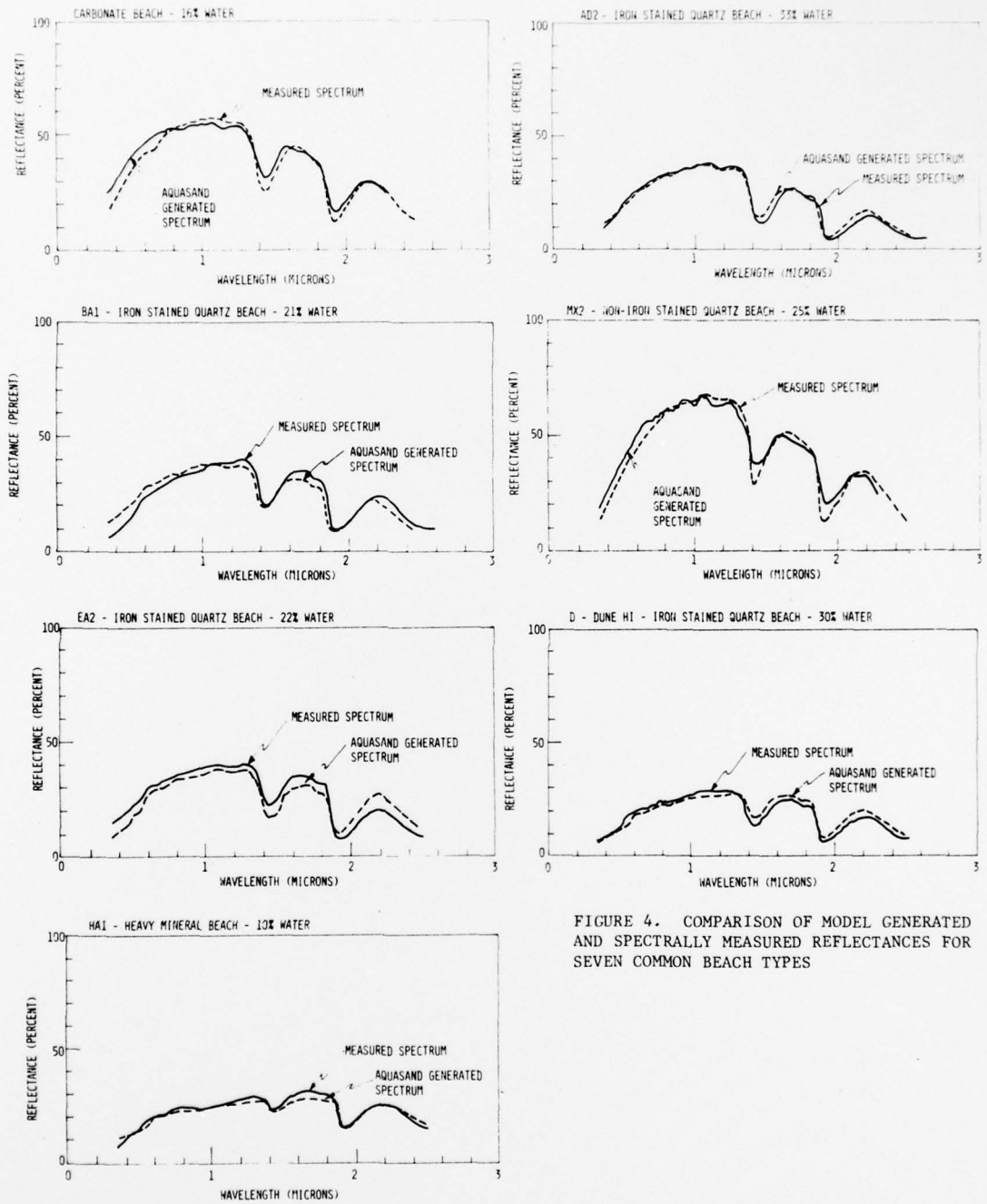


FIGURE 4. COMPARISON OF MODEL GENERATED AND SPECTRALLY MEASURED REFLECTANCES FOR SEVEN COMMON BEACH TYPES

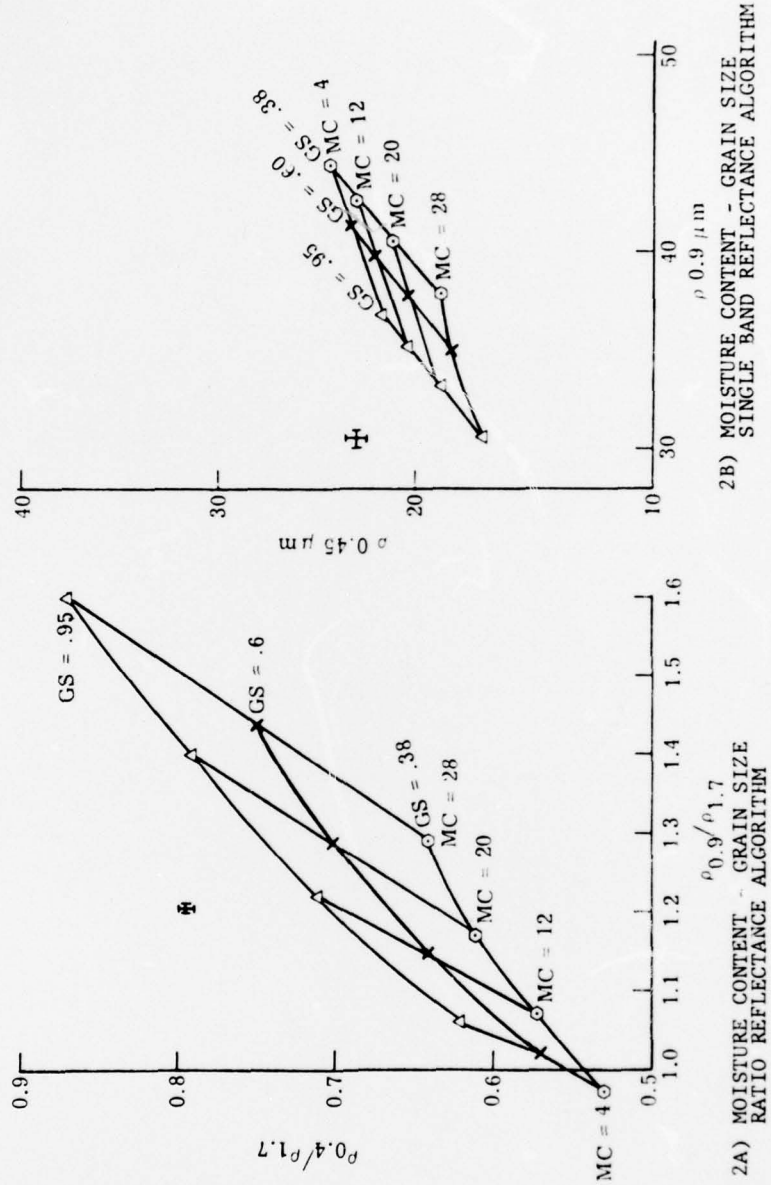


FIGURE 5. RATIO REFLECTANCE AND SINGLE BAND ALGORITHMS FOR SEPARATING MOISTURE AND GRAIN SIZE.

APPENDIX B

SIMULATION OF MOISTURE VARIATION
IN THE AQUASAND MODEL

APPENDIX B
SIMULATION OF MOISTURE VARIATION
IN THE AQUASAND MODEL

Before a wet sand can be modeled, an understanding of how water is incorporated into the sand must be reached. Besides a dry sand, a saturated sand is the easiest to model. In a saturated sand, water fills all the voids which are, in a dry sand, air spaces between the sand grains. For such a case the AQUASAND model includes the absorption coefficient of water in the optical pathway equations. Because AQUASAND calculates the reflectance of a modeled sand at discrete wavelength intervals (0.01 μm increments), the water absorption coefficients must be entered into the model in the same intervals. Another dry-sand to wet-sand change that must be considered is that the index of refraction difference between sand particles and water air is smaller than the equivalent difference from sand particles to air. Since surface reflectance from particles is governed by the difference in index of refraction from one medium to another, less reflectance and more transmittance is noted for saturated sand as compared to dry sand. The AQUASAND model allows different indices of refraction to be used depending on the intergrain medium.

Sands are most commonly found to be somewhere between dry and saturated in a coastal situation. In such cases there is a combination of air and water in the void spaces between the sand grains. The model treats the air portion of this combination as being granular in the sense that bubbles may be thought of as being air grains in a matrix of water. Using this logic, these air grains are treated as another particle type within the sand. Based on the index of refraction difference between water and air, each bubble has a transmittance of 58% and a reflectance of 42%. There is, of course, no absorption associated with air bubbles.

As was described in Appendix A, the AQUASAND model looks at granular beach constituents. As being orthogonal Lambertian panel. Each panel represents either the horizontal (parallel to the beach surface) or vertical

(perpendicular to the beach surface) component of an associated grain. The size of each panel is determined by the size of the associated sand grain. Each air bubble in a wet sand is treated in this same way. The size of air bubble and the associated panels is dependent on the amount of void space not occupied by water. The number of air bubbles in any given volume of sand is assumed to be equal to the number of grains of sand in that volume. Therefore, the volume of each air bubble is,

$$V_{\text{bubble}} = \frac{VS_{\text{air/cm}^2}}{\text{No. sand grains/cm}^2},$$

where VS_{air} is the void space not occupied by water. Once the bubble volume is computed, the horizontal and vertical components of each bubble may be determined.

By using the above rationale the model implements the same procedure to calculate the reflectance of any wet sand throughout the entire range of potential moisture contents. For high moisture contents the bubbles are small and the water fraction is large, and for low moistures the opposite is true. When the moisture content decreases to the point where the amount of water coating the sand grains is on the order of one wavelength thick, the sand is said to be dry. The model recognizes this situation by the equation:

$$WT = \frac{\text{Volume of water/cm}^3 \text{ sand}}{\text{Total surface area of sand grains/cm}^3 \text{ sand}},$$

where WT is the average water thickness coating the sand grains. When WT decreases to a depth of 1 wavelength all the water terms are removed from the optical pathway equations and the sand is treated as being dry. In fact, the water will give diffraction effects down to a thickness of 1/4 wavelength (similar to that noted with a light oil slick on water), however, this does not appear to alter the bulk reflectance significantly.

BIBLIOGRAPHY

1. Vincent, R.K., Rock-type discrimination from ratio images of the Pisgah Crater, California test site, The University of Michigan, Report No. 3165-77-T, NASA Contract NAS9-9784, 1972.
2. Vincent, R.K., A thermal infrared ratio imaging method for mapping compositional variations among silicate rock types, unpublished PhD dissertation, The University of Michigan, 1973.
3. Vincent, R.K. and F.J. Thomson, Spectral compositional imaging of silicate rocks, *Journal of Geophys. Res.*, Vol. 77, 1972, pp. 2465-2471.
4. Vincent, R.K., F.J. Thomson and K. Watson, Recognition of exposed quartz sand and sandstone by two-channel infrared imagery, *J. of Geophys. Res.*, Vol. 77, 1972, pp. 2473-2477.
5. Watson, R.D., Surface-coating effects in remote sensing measurements, *J. of Geophys. Res.*, Vol. 75, 1970, pp. 480-484.
6. Hovis, W.A. and W.R. Callahan, Infrared reflectance spectra of igneous rocks, tuffs, and red sandstone from 0.5 to 22 μm , *J. of the Opt. Soc. of Am.*, Vol. 56, No. 5, 1966, pp. 639-643.
7. Vincent, R.K. and G.R. Hunt, Infrared reflectance from mat surfaces, *Applied Optics*, Vol. 7, No. 1, 1958, pp. 53-59.
8. Hunt, G.R. and R.K. Vincent, The behavior of spectral features in the infrared emission from particulate surfaces of various grain sizes, *J. of Geophys. Res.*, Vol. 73, No. 18, 1968, pp. 6039-6046.
9. Shuchman, R.A., G.H. Suits, and C.F. Davis, 1978, AQUASAND: A beach reflectance model and validation tests, paper presented at Fifth Canadian Symposium on Remote Sensing of the Environment, August 26-30, Victoria, British Columbia, Canada
10. Hunt, G.R. and J.W. Salisbury, Visible and near infrared spectra of minerals and rocks: I silicate minerals, *Modern Geology*, Vol. 1, 1970, pp. 283-300.
11. Thomson, F., R. Shuchman, C. Wezernak, D. Lyzenga, and D. Leu, Basic remote sensing investigation for beach reconnaissance, Report 108900-5-P, Environmental Research Institute of Michigan, Ann Arbor, Michigan, July 1976.
12. Williams, J., *Optical properties of sea*, Naval Institute Press, 1970. 123 p.

DISTRIBUTION LIST

Office of Naval Research Geography Programs Code 462 Arlington, Virginia 22217	2 copies	ONR Scientific Liaison Group American Embassy - Room A-407 APO San Francisco 96503
Defense Documentation Center Cameron Station Alexandria, Virginia 22314	12 copies	Commander Naval Oceanographic Office Attention: Library Code 1600 Washington, D.C. 20374
Director, Naval Research Lab Attention: Technical Information Officer Washington, D.C. 20375	6 copies	Naval Oceanographic Office Code 3001 Washington, D.C. 20374
Director, Office of Naval Research Branch Office 1030 East Green Street Pasadena, California 91101		Chief of Naval Operations OP 987P1 Department of the Navy Washington, D.C. 20350
Director, Office of Naval Research Branch Office 536 South Clark Street Chicago, Illinois 60605		Oceanographer of the Navy Hoffman II Building 200 Stovall Street Alexandria, Virginia 22322
Director, Office of Naval Research Branch Office 495 Summer Street Boston, Massachusetts 02210		Naval Academy Library U.S. Naval Academy Annapolis, Maryland 21402
Commanding Officer Office of Naval Research Branch Office Box 39 FPO New York 09510		Commanding Officer Naval Coastal Systems Laboratory Panama City, Florida 32401
Chief of Naval Research Asst. for Marine Corps Matters Code 100M Office of Naval Research Arlington, Virginia 22217		Librarian Naval Intelligence Support Center 4301 Suitland Road Washington, D.C. 20390
NORDA Code 400 National Space Technology Laboratories Bay St. Louis, Mississippi 39520		Officer in Charge Environmental Research Prdctn. Felty. Naval Postgraduate School Monterey, California 93940
Office of Naval Research Operational Applications Division Code 200 Arlington, Virginia 22217		Commanding General Marine Corps Development and Educational Command Quantico, Virginia 22134
Office of Naval Research Scientific Liaison Officer Scripps Institution of Oceanography La Jolla, California 92093		Dr. A. L. Slafkosky Scientific Advisor Commandant of the Marine Corps Code MC-RD-1 Washington, D.C. 20380
Director, Naval Research Laboratory Attention: Library, Code 2628 Washington, D.C. 20375		Defense Intelligence Agency Central Reference Division Code RDS-3 Washington, D.C. 20301



Director
Defense Mapping Topographic Center
Attention: Code 50200
Washington, D.C. 20315

Commanding Officer
U.S. Army Engineering
Topographic Laboratory
Attention: ETL-ST
Fort Belvoir, Virginia 22060

Chief, Wave Dynamics Division
USAE-WES
P.O. Box 631
Vicksburg, Mississippi 39180

National Oceanographic Data
Center D764
Environmental Data Services
NOAA
Washington, D.C. 20235

Central Intelligence Agency
Attention: OCR/DD-Publications
Washington, D.C. 20505

Dr. Mark M. Macomber
Advanced Technology Division
Defense Mapping Agency
Naval Observatory
Washington, D.C. 20390

Ministerialrat Dr. F. Wever
RUE/FO
Bundesministerium der Verteidigung
Hardthoehe
D-5300 Bonn, West Germany

Oberregierungsrat Dr. Ullrich
Rue/FO
Bundesministerium der Verteidigung
Hardthoehe
D-5300 Bonn, West Germany

Mr. Tage Strarup
Defence Research Establishment
Osterbrogades Kaserne
DK-2100 Koberhavn O, Denmark

IR. M. W. Van Batenberg
Physisch Laborarium INO
Oude Wallsdorper Weg 63, Den Haag
Netherlands

Dr. Gordon E. Carlson
University of Missouri
Department of Electrical Engineering
Rolla, Missouri 65401

Coastal Studies Institute
Louisiana State University
Baton Rouge, Louisiana 70803

Dr. Bernard Le Mehaute
Tetra Tech. Inc.
630 North Rosemead Boulevard
Pasadena, California 91107

Dr. William S. Gaither
Dean, College of Marine Studies
Robinson Hall
University of Delaware
Newark, Delaware 19711

Dr. Lester A. Gerhardt
Rennselaer Polytechnic Institute
Troy, New York 12181

Dr. Thomas K. Peucker
Simon Fraser University
Department of Geography
Burnaby 2, B.C., Canada

Dr. Bruce Hayden
Department of Environmental Sciences
University of Virginia
Charlottesville, Virginia 22903